In Vivo Prediction of Air-Puff Induced Corneal Deformation Using LASIK, SMILE, and PRK Finite Element Simulations

Mathew Francis,[1] Pooja Khamar,[2] Rohit Shetty,[2] Kanchan Sainani,[2] Rudy M. M. A. Nuijts,[3] Bart Haex,[4] and Abhijit Sinha Roy[1]

[1]Imaging, Biomechanics and Mathematical Modeling Solutions Lab, Narayana Nethralaya Foundation, Bangalore, India
[2]Department of Cornea and Refractive Surgery, Narayana Nethralaya, Bangalore, India
[3]University Eye Clinic Maastricht, Maastricht University Medical Center, Maastricht, The Netherlands
[4]Director of Research Policy, Maastricht University, Maastricht, The Netherlands

Correspondence: Mathew Francis, Narayana Nethralaya, #258A Hosur Road, Bommasandra, Bangalore 560099, India; mathewbme@gmail.com.

MF, PK, and RS contributed equally to the work presented here and should therefore be regarded as equivalent authors.

Submitted: April 21, 2018
Accepted: October 1, 2018

Citation: Francis M, Khamar P, Shetty R, et al. In vivo prediction of air-puff induced corneal deformation using LASIK, SMILE, and PRK finite element simulations. *Invest Ophthalmol Vis Sci*. 2018;59:5320–5328. https://doi.org/10.1167/iovs.18-24470

Purpose. To simulate deformation amplitude after laser-assisted in situ keratomileusis (LASIK), small incision lenticule extraction (SMILE), and photorefractive keratectomy (PRK) with finite element models.

Methods. Finite element simulations of air-puff applanation on LASIK, SMILE, and PRK models were performed on a cohort of normal eyes, which had undergone refractive treatments. Short- and long-term wound healing responses were considered for SMILE and LASIK models based on evidence of microdistortions in Bowman's layer and crimping of collagen fibers. First, inverse simulations were performed to derive the preoperative properties of the cornea. Using these properties and planned refractive treatment, postoperative air-puff deformation amplitude was predicted and compared with the in vivo measurements.

Results. The predicted postoperative corneal stiffness parameters agreed very well with in vivo values of SMILE, LASIK, and PRK eyes. Intraclass correlations (ICC) were greatest in PRK eyes (ICC $>$ 0.95). This agreement was lower for peak deformation amplitude and peak deflection amplitude in SMILE and LASIK eyes (ICC $<$ 0.9). In PRK eyes, peak deformation and deflection amplitude predictions were the best relative to in vivo magnitudes. Also, linear correlation (r) between in vivo measurement and predicted biomechanical parameters indicated strong agreement between them (SMILE: $r \geq 0.89$, LASIK: $r \geq 0.83$, PRK: $r \geq 0.87$).

Conclusions. The is the first study to present predictive simulations of corneal deformation changes after different procedures. Patient-specific preoperative corneal biomechanical properties and finite element models were a significant determinant of accurate postoperative deformation amplitude prediction.

Keywords: cornea, SMILE, LASIK, PRK, finite, element modeling, prediction

The anterior stroma of the cornea has an interweaving network of collagen fibers around the collagen lamellae.[1] This interweaving progressively becomes less through the depth of the stroma.[1] These structural features could be responsible for the greater tensile strength of the anterior stroma relative to the posterior stroma.[2] There are procedures that significantly alter the anterior stroma, such as laser-assisted in situ keratomileusis (LASIK) and photorefractive keratectomy (PRK). In PRK, a portion of the anterior stroma is ablated in comparison to LASIK. Small incision lenticule extraction (SMILE) is another refractive procedure, which leaves much of the anterior stroma intact compared to LASIK and PRK. Using theoretical models, it was concluded that corneas undergoing SMILE could be biomechanically stronger compared to LASIK and PRK postoperatively.[3,4]

Air-puff applanation is the only clinical method available to assess corneal biomechanics. However, clinical studies on biomechanical changes in the cornea after these procedures were inconclusive.[5–7] Using dynamic air-puff applanation, two studies indicated a better biomechanical result after PRK than after LASIK.[5,6] Another study reported similar outcomes between PRK and LASIK.[3] However, a theoretical model predicted better biomechanical outcomes after SMILE and LASIK than after PRK.[3] Recent clinical data demonstrated equivalence between SMILE and LASIK with respect to biomechanical changes in the cornea after surgery.[8–10] Further, Corvis-ST (OCULUS Optikgerate Gmbh, Wetzlar, Germany) was an improved device over the Ocular Response Analyzer (Reichert, Inc., Depew, NY, USA) since it had a highly repeatable pressure profile and quantified the mechanical deformation of the cornea. Theoretical models showed that LASIK caused a greater increase in mechanical stress in the residual stromal bed than SMILE.[4] Therefore, this study investigated simulated air-puff applanation on LASIK, PRK, and SMILE finite element models, using the pressure profile generated by Corvis-ST.[11] In the finite element models, the transient air puff was exported from Corvis-ST dynamic Scheimpflug analyzer and spatially distributed on the anterior surface using fluid dynamics analysis.[11]

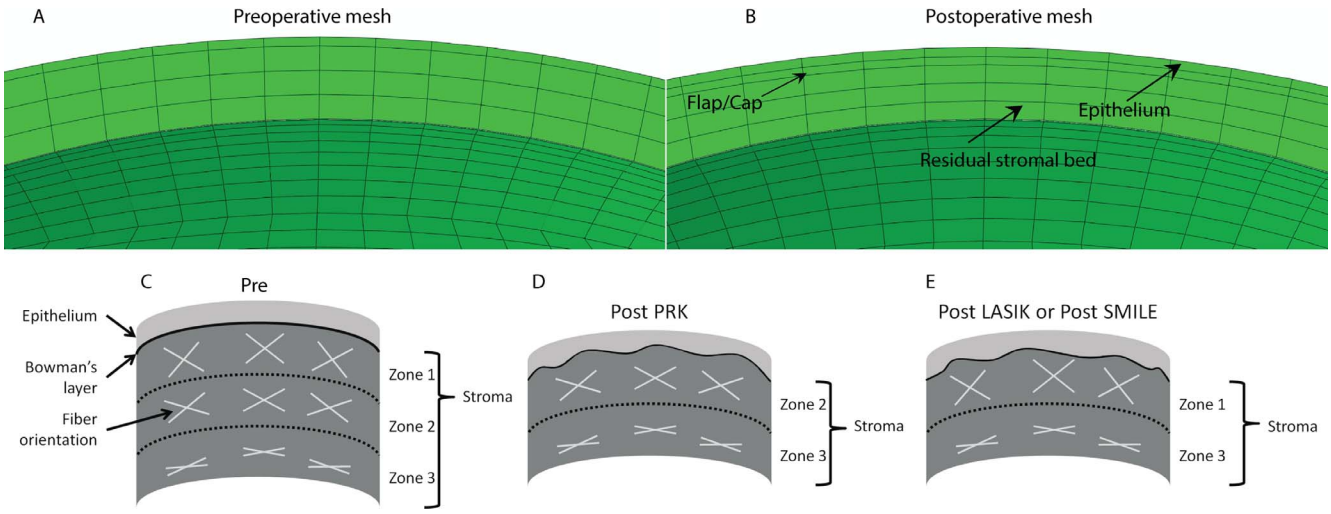

Figure 1. A cross section of the finite element mesh: (**A**) preoperative and (**B**) postoperative. A schematic of preoperative (**C**), post PRK (**D**), and post SMILE or LASIK (**E**) distribution of interweaving collagen fibers through the depth of the corneal stroma. For simplicity, zone 1 was considered as the flap and cap region of the central cornea in LASIK (**E**) and SMILE (**E**) models, respectively. Zone 2 was the zone of tissue removed (**E**) during simulated SMILE and LASIK. Zone 3 was the residual stromal bed. In PRK, zone 1 was the zone of tissue ablated, leaving zones 2 and 3 as the residual stromal bed (**D**). These schematics show the differences in the fiber distributions through the depth of the stroma in the postoperative finite element models.

Methods

This was a simulation study using finite element modeling. The method for the finite element model generation is briefly described here from another recent study.[11] Three-dimensional (3-D) geometry of a patient cornea was created from Pentacam (OCULUS Optikgerate Gmbh). The Pentacam provided Cartesian coordinates of the anterior and posterior corneal surface, which were used for creating a 3-D volume. Epithelium thickness of the cornea was measured with RTVue (Optovue, Inc., Fremont, CA, USA). Finite element mesh was created with 8-noded linear hexahedral elements (TrueGrid; XYZ Scientific Applications, Inc., Livermore, CA, USA). A total of 3312 hexahedral elements were used to represent the corneal volume. Figures 1A and 1B show a cross section of the preoperative and postoperative mesh (with flap/cap) of the central cornea, respectively. PRK finite element mesh did not have any flap/cap zone. An anisotropic, hyperelastic, fiber-dependent material model with material incompressibility was chosen.[1] The material model accounted for the orthogonal arrangement of fibers in the central cornea, depth dependency of angular direction of the interweaving fibers, and reorientation of the in-plane peripheral collagen fibers to circumferential direction.[11] The hyperelastic material model was represented by free energy density (ψ):

$$\psi(C) = \psi_m(I_1, I_3) + \psi_{f\text{-}plane}(C) + \psi_{f\text{-}cross}(C) \qquad (1)$$

where $I_1 = \mathrm{C} : 1$ and $I_3 = \det[C]$ were the 1st and 3rd invariants of the deformation tensor. C was the right Cauchy-Green deformation tensor and $\det[C]$ represented determinant of the tensor. The isotropic energy density of the matrix (ψ_m) was described by:

$$\psi_m(I_1, I_3) = C_1(\bar{I}_1 - 3) + C_2(\bar{I}_1 - 3)^2 + \frac{(I_3 - 1)^2}{D_1} \qquad (2)$$

where $\bar{I}_1 = I_3^{-1/3} I_1$ was the distortional part of I_1, I_3 was the determinant of deformation gradient tensor, and C_1s were the material constants. D_1 was the bulk modulus to enforce incompressibility and was assumed to be 10^{-6}. The fiber energy density ($\psi_{f\text{-}plane}$) was described by:

$$\psi_{f\text{-}plane}(C) = \int_{-\pi}^{\pi} W_f\left(\lambda_{f\text{-}plane}\right) D_{plane}(\theta)\, d\theta \qquad (3)$$

$$W_{f\text{-}plane}\left(\lambda_{f\text{-}plane}\right) = \frac{k_1}{2k_2} \exp\left(k_2\left[\lambda_{f\text{-}plane} - 1\right]^2\right) - \frac{k_1}{2k_2} \qquad (4)$$

$\psi_{f\text{-}plane}$ represented the energy density of in-plane lamellar collagen fibers with stretch, $\lambda_{f\text{-}plane}$ equal to $\sqrt{A.CA}$, where $A = [\cos\theta, \sin\theta, 0]^T$ was the local direction vector of the fibers. k_1 and k_2 were the material constants. $D_{plane}(\theta)$ represented a weighted average of the energy density of the fiber families at each integration point of the element. It also represented the change in the preferred direction of the fibers from orthogonal in the central cornea to circumferential near the limbus.

$$\psi_{f\text{-}cross}(C) = \int_{-\pi}^{\pi} W_f\left(\lambda_{f\text{-}cross}\right) D_{cross}(\theta)\, d\theta \qquad (5)$$

$$W_{f\text{-}cross}\left(\lambda_{f\text{-}cross}\right) = \frac{k_1}{2k_2} \exp\left(k_2\left[\lambda_{f\text{-}cross} - 1\right]^2\right) - \frac{k_1}{2k_2} \qquad (6)$$

$\psi_{f\text{-}cross}$ represented the energy density of crosslink fibers between the lamellae with stretch, $\lambda_{f\text{-}cross}$ equal to $\sqrt{B.CB}$, where B was the direction vector of the crosslink fibers. B was determined by taking a cross-product of A with the surface normal and then rotating it out-of-plane around A by an angle ξ. The angle ξ was assumed to be a function of depth and was modeled as follows[11]:

$$\xi = 28.6^{\circ} \frac{\exp(3.19[1 - s]) - 1}{\exp(3.19) - 1} \qquad (7)$$

s was the nondimensional local thickness. The angle ξ was evaluated at each element centroid. $D_{plane}(\theta)$ was kept equal to $D_{cross}(\theta)$. From the above equations, the Cauchy stress was determined by:

$$\sigma = \frac{1}{\sqrt{I_3}} F \frac{\partial \psi}{\partial C} F^T \qquad (8)$$

where F was the deformation gradient tensor. The epithelium was modeled as an isotropic, hyperelastic, incompressible material [$\psi(C) = \psi_m(I_1, I_3)$ only] with $c_1 = 5$ kPa (Pascal) and $c_2 = 0.0$ kPa.

To derive the in vivo anisotropic material properties of the cornea, deformation amplitude measurement (from Corvis-ST) of the patient was coupled with an inverse finite element model.[11] The inverse finite element model derived the in situ corneal (C_1, C_2, k_1, and k_2) and extracorneal [Kz (N/m), μ (Pa.sec), and m (gm)] material properties. The inverse model minimized the difference between the measured displacements of the anterior edge of the cornea and calculated displacements of the same edge from the finite element simulations. The inverse model was designed such that the corneal and extracorneal properties were governed by the corneal deformation (reported as deflection amplitude by Corvis-ST) and whole-eye movement, respectively.[11] Here, deformation amplitude was the arithmetic sum of corneal deformation and whole-eye movement.[11] An iterative method (Levenberg–Marquardt algorithm) for minimization was adopted. The finite element simulations were performed in ABAQUS (Dassault Systèmes Americas Corporation, Waltham, MA, USA). The material model was incorporated in the simulations using ABAQUS material subroutine (UMAT). The inverse calculations were performed using a custom script written in Python (v2.7.3). ABAQUS simulations and Python scripts were executed simultaneously in a multithreaded workstation.

To simulate a myopic spherical power correction, the anterior surface of the corneal geometry was recomputed using an aspheric ablation profile.[12] Figure 1C shows a schematic of a cross section of the cornea (epithelium and stroma). The figure shows the epithelium, flap in LASIK (or cap in SMILE), peripheral cornea outside the flap/cap and the residual stromal bed. For simplicity, the stroma was further subdivided into three zones in the axial direction for better visualization of the angular orientation of the interweaving fibers. As shown in Figure 1C, the angular direction of the interweaving fibers decreased through the depth of the stroma; that is, zone 1 (anterior stroma) was the stiffest followed by zones 2 and 3.[1] Different surgical procedures were simulated as follows.

PRK: In PRK, a significant portion of the anterior stroma was removed from the corneal 3-D geometry, which depended on the magnitude of myopic correction. This can be visualized in Figure 1D, where zone 1 of the stroma was removed to simulate the refractive change. Thus, the corneal geometry had residual interweaving collagen fibers with angular orientation of zones 2 and 3 with reference to preoperative structure (Fig. 1C). Also, it was assumed that epithelium remodeling was complete after the simulated surgery. It was also assumed that the preoperative and postoperative epithelium thicknesses were the same. The optical diameter of the ablation profile and the treatment zone was 6 and 9 mm, respectively.[12]

SMILE: Figure 1E shows a schematic of a cross section of the cornea with simulated SMILE. The anterior surface of the cornea geometry was altered with aspheric ablation profile. For simplicity, let's assume that zone 1 was the cap and zone 2 was the region of the stroma corresponding to the SMILE lenticule. Thus, zone 2 would be absent after simulated SMILE. The corneal geometry would retain only zones 1 and 3 with corresponding angular directions of the interweaving fiber as shown in Figure 1C. Here, zone 3 was the residual stroma bed (RSB). In the simulated finite element model, the cap and RSB were modeled explicitly. Further, a discontinuity in the transition of the angular direction of interweaving fibers was modeled between the cap and RSB (as shown schematically in Fig. 1B) in the ABAQUS user subroutine. The simulated optical and cap diameter were 6 mm and 7.8 mm, respectively.

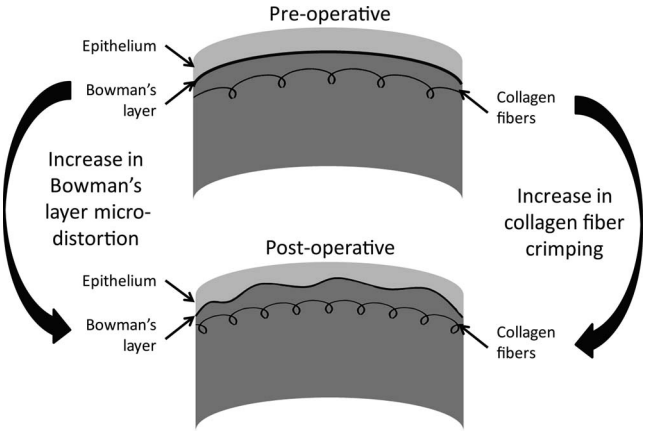

FIGURE 2. A model to describe preoperative and postoperative structure of Bowman's layer and collagen fiber in stroma. Due to surgery, microdistortions in the Bowman's layer increase due to compression of the cap/flap. This may result in crimping of the collagen fibers; that is, fibers are under reduced tension and may not bear the stress due to intraocular pressure.

To model the postoperative mechanics of the cap, a short- and long-term wound healing response was hypothesized. While wound healing is a broad topic involving changes in hydration and keratocytes among other physiological components, we evaluated the recruitment of the collagen fibers to bear mechanical stress only in this study as wound healing response. Increased microdistortions were detected in the Bowman's layer after SMILE, which did not resolve even up to 3 months after the surgery.[13] This increase in microdistortions could be indicative of compression of the cap due to mechanical extraction of the lenticule and mismatch between the lenticular surfaces.[13] This directly implied that the collagen fibers in the cap were probably under reduced tensile stress and underwent some crimping[14] since the microdistortions were greater than in the preoperative state even 3 months after SMILE (Fig. 2). Therefore, the cap was assumed to have only isotropic material properties (C_1 and C_2 were the same as preoperative, k_1 and k_2 were set to zero) in the finite element model assuming short-term wound healing. In the long-term finite element model, the cap material properties were set the same as preoperative anisotropic, hyperelastic properties with the assumption that incision in the anterior stroma did not cause a significant decrease in the cap's strength. Further, the postoperative material properties and fiber distributions of the peripheral cornea outside the cap zone were assumed to be the same as preoperative state.

LASIK: The difference between SMILE and LASIK is the presence of the flap instead of a cap. The flap has an arc span of nearly 360°. By extrapolating the effect of crimping of collagen fibers in the cap, it was logical to assume that the flap also should undergo a similar change; that is, the collagen fibers were under reduced tension (Fig. 2). In the finite element model, the angular orientation of the interweaving fibers in the LASIK model would be similar to the SMILE model (Fig. 1C). However, the short- and long-term finite element model of LASIK assumed only isotropic material properties for the flap since the LASIK flap cut severed a significantly greater number of collagen fibers in the anterior stroma and it was unlikely that these severed fibers reattached to the RSB. The simulated optical and cap diameter were 6 mm and 9.0 mm, respectively. The epithelium thickness in the LASIK model was assumed to be the same as preoperative state. The postoperative material properties (including the fiber distributions) of

Table 1. Mean [95% Confidence Interval] of Preoperative Demographics (Column 1) of the Cohorts

	SMILE, $n = 12$	LASIK, $n = 12$	PRK, $n = 12$	P Value
In vivo preoperative CCT, μm	504 [481.3 to 526.7]	511.9 [489.7 to 534.2]	515 [497 to 533]	0.90
In vivo postoperative CCT, μm	452.8 [439.3 to 466.3]	460.8 [438.6 to 483]	459.3 [426 to 492.5]	0.87
Predicted CCT, μm	457.4 [444.8 to 469.9]	464.8 [443.3 to 486.3]	465.5 [431.6 to 499.5]	0.85
Intraocular pressure, mm Hg	16.25 [15.55 to 16.95]	16.17 [15.41 to 16.93]	17.2 [15.83 to 18.51]	0.80
Manifest refraction spherical equivalent, D	−4.75 [−5.66 to −3.84]	−4.67 [−5.58 to −3.75]	−4.27 [−5.44 to −3.1]	0.84

peripheral cornea outside the flap zone and in the RSB were assumed to be the same as preoperative state.

Postoperatively, the peripheral lamellae, adjacent to the flap/cap, were assumed to be in continuum with the lamellae of the RSB similarly to the preoperative state. Further, simulated flap/cap thicknesses included the epithelium thicknesses.

The validation of the surgical finite element simulations on the model eye was conducted in two phases. In the first phase, the model results were compared with clinical outcomes of cohorts of eyes that underwent LASIK, SMILE, and PRK. The prediction of Kc (constant), Kc (mean), peak deformation amplitude, and peak deflection amplitude was performed for the cohort of eyes. The corneal stiffnesses, Kc (constant), and Kc (mean) were calculated from the deformation amplitude using an analytical approach.[15,16] First, the preoperative material properties of each eye were determined with the inverse finite element method described earlier. The programmed refractive error (sphere and cylindrical error) was simulated in the finite element mesh with aspheric profile. Then, postoperative deformation amplitude of each eye was simulated with its respective surgical model, that is, LASIK, PRK, or SMILE. The peak deformation amplitude and Kc (constant) was determined from the computed postoperative deformation amplitude. The "short-term wound healing" assumption was applied to the postoperative finite element simulations. These were compared with the same derived from in vivo measurement of postoperative deformation amplitude. In the second phase, a case example of one eye from each group with similar preoperative IOP and central corneal thickness (CCT) was chosen. In other words, validation was conducted both for a cohort of eyes and a set of individual eyes. For the cohort of eyes, root mean square error (RMSE) was calculated for each parameter within a group, for example, RMSE of Kc (constant) for SMILE eyes was square root of sum of squares of difference between in vivo and predicted magnitude of Kc (constant) divided by total number of eyes that underwent SMILE.

This was a retrospective analysis of data. The study was approved by ethics committee of the Narayana Nethralaya Eye Hospital, Bangalore, India. The study adhered to the tenets of Declaration of Helsinki. All the surgeries were performed by a single experienced surgeon under topical anesthesia using 0.5% proparacaine hydrochloride (Paracain; Sunways Pvt. Ltd., Mumbai, India) instilled two or three times. LASIK was performed with the WaveLight FS200 femtosecond laser and WaveLight EX500 excimer laser platform (Alcon Laboratories, Fort Worth, TX, USA). A flap (9.0-mm diameter, 110-μm thickness, a side cut angle of 70°, canal width of 1.5 mm, and hinge position at 90°) was created. After the flap was created, the same was manually lifted and excimer ablation of targeted refraction was performed. SMILE was performed with the VisuMax femtosecond laser system (Carl Zeiss Meditec AG, Jena, Germany). Cap thickness was 110 μm. Lenticule and cap diameter were 6.0 and 7.8 mm, respectively. These flap and gap geometric details were incorporated in the 3-D finite element model. After creation of the refractive lenticule, it was dissected and extracted manually through a superior 3-mm side cut. Cornea was remoistened with a wet Merocel sponge at the end of the procedure. After the surgery, one drop of moxifloxacin hydrochloride 0.5% (Vigamox; Alcon Laboratories) was applied to both eyes.

All PRK procedures were done under 0.5% proparacaine hydrochloride and strict aseptic conditions. The epithelium was manually scraped in the central 8-mm-diameter zone before ablation. Wavefront optimized PRK was performed with WaveLight Allegretto EX 500 laser (Alcon Laboratories) using a 6-mm-diameter optical zone. A bandage contact lens (Ciba Vision, Duluth, MN, USA) was applied after the surgery. Routine postoperative regimen was followed for all eyes. This included moxifloxacin hydrochloride 0.5% eye drops (Vigamox, Alcon Laboratories) four times a day for 1 week, tapering doses of topical 1% fluorometholone eye drops (Flarex, Alcon Laboratories), and topical lubricants (Optive; Allergan, Inc., Irvine, CA, USA) four times a day for 3 months. All eyes underwent Corvis-ST measurement before and 3 months after surgery. The preoperative and postoperative deformation amplitude of each eye was analyzed to determine peak deformation amplitude and with the analytical model to determine Kc (constant). These were compared with the results of simulations on the model eye. Mean deformation amplitude of each cohort of eyes was compared between preoperative and postoperative time points. Deformation amplitude was chosen as the primary comparator since it allowed easy visual comparison between in vivo and simulation results.

Results

Table 1 shows the preoperative demographics of the three cohorts of eyes. A comparison of the in vivo postoperative and simulated central corneal thickness in the postoperative finite element geometry is also shown in Table 1. All groups were statistically similar preoperatively ($P > 0.05$). Table 2 shows the in vivo preoperative and postoperative Kc (mean), Kc (constant), peak deformation amplitude, and peak deflection amplitude. The predicted magnitudes of the above variables are also shown in Table 2. There was excellent agreement between measured and predicted magnitudes of Kc (mean) and Kc (constant) since intraclass correlation (ICC) was greater than 0.9 for all procedures. Overall, prediction of peak deformation amplitude and deflection amplitude was best in PRK eyes (ICC $\sim$ 0.9), which could be due to absence of flap or cap in PRK. However, the difference between in vivo preoperative and in vivo postoperative peak deformation and deflection amplitude was similar between all the eye groups (Table 2). RMSE of Kc (mean) and Kc (constant) were significantly greater than the difference between the mean values of in vivo and predicted postoperative magnitudes (Table 2). This explained the high ICC for Kc (mean) and Kc (constant) for SMILE, LASIK, and PRK eyes. Interestingly, RMSE of peak deformation and deflection amplitude were within

Table 2. In Vivo (Preoperative and Postoperative) and Predicted (Only Postoperative) Values of Corneal Stiffness, Peak Deformation, and Peak Deflection Amplitude for SMILE, LASIK, and PRK Eyes ($n = 12$ Eyes per Surgery). Values Are Reported as Mean [95% Confidence Interval] of the Mean

Parameter	In Vivo Preoperative Measurement	In Vivo Postoperative Measurement*	Predicted Postoperative Value*	Intraclass Correlation*	RMSE of Prediction
SMILE					
Kc (mean), N/m	101.35 [92.83–109.86]	86.13 [80.98–91.28]	87.9 [81.95–93.85]	0.95	3.53
Kc (constant), N/m	104.01 [97.72–110.3]	92.79 [88.63–96.95]	90.26 [86.52–94]	0.93	3.15
Peak deformation amplitude, mm	1.15 [1.09–1.21]	1.23 [1.16–1.3]	1.29 [1.24–1.34]	0.81	0.08
Peak deflection amplitude, mm	1.02 [0.96–1.07]	1.08 [1.03–1.14]	1.16 [1.11–1.21]	0.72	0.09
LASIK					
Kc (mean), N/m	101.05 [95.11–106.99]	91.32 [84.52–98.13]	91.56 [85.29–97.83]	0.95	3.55
Kc (constant), N/m	104.9 [98.85–110.96]	96.01 [88.18–103.85]	93.83 [87.63–100.04]	0.96	3.37
Peak deformation amplitude, mm	1.13 [1.07–1.19]	1.21 [1.12–1.31]	1.26 [1.18–1.34]	0.91	0.07
Peak deflection amplitude, mm	1.03 [0.96–1.1]	1.08 [1.02–1.15]	1.18 [1.08–1.27]	0.73	0.11
PRK					
Kc (mean), N/m	96.78 [85.64–107.92]	90.43 [77.58–103.29]	87.27 [73.86–100.69]	0.99	3.49
Kc (constant), N/m	101.28 [93.5–109.07]	96.24 [87.25–105.22]	91.77 [81.77–101.77]	0.96	4.84
Peak deformation amplitude, mm	1.17 [1.05–1.29]	1.23 [1.12–1.33]	1.28 [1.15–1.41]	0.91	0.09
Peak deflection amplitude, mm	1.02 [0.93–1.12]	1.07 [0.97–1.17]	1.17 [1.03–1.3]	0.89	0.12

* Indicates corresponding intraclass correlation between magnitudes reported in columns 3 and 4.

repeatability of these parameters.[17,18] Further, PRK eyes had the least decrease in magnitude of Kc (mean) and Kc (constant) after surgery; for example, in vivo mean Kc (mean) and mean Kc (constant) decreased by 6.35 and 5.04 N/m only (Table 2). In contrast, LASIK and SMILE caused a greater decrease in stiffnesses (Table 2).

Overall, PRK eyes had the best agreement (ICC $\sim$ 0.9 and above) between in vivo postoperative measurement and predicted postoperative value (Table 2). Figure 3 shows an overlay of the mean deformation amplitude of the eyes before and after surgery from LASIK, SMILE, and PRK cohorts. These waveforms were derived by averaging the in vivo deformation amplitude waveforms of all the eyes at respective time points for a given treatment (LASIK, SMILE, or PRK). Linear regression analyses (Table 3) were performed between the in vivo and predicted postoperative variables for all the 36 eyes (taken together) and separate cohorts. From Table 3, the correlation coefficients (r) were 0.95, 0.94, 0.87, and 0.90 for Kc (mean), Kc (constant), peak deformation amplitude, and peak deflection amplitude, respectively, for all eyes ($n = 36$). The slopes of the linear regressions were 0.93, 0.91, 0.81, and 0.70, respectively ($P < 0.001$ for all).

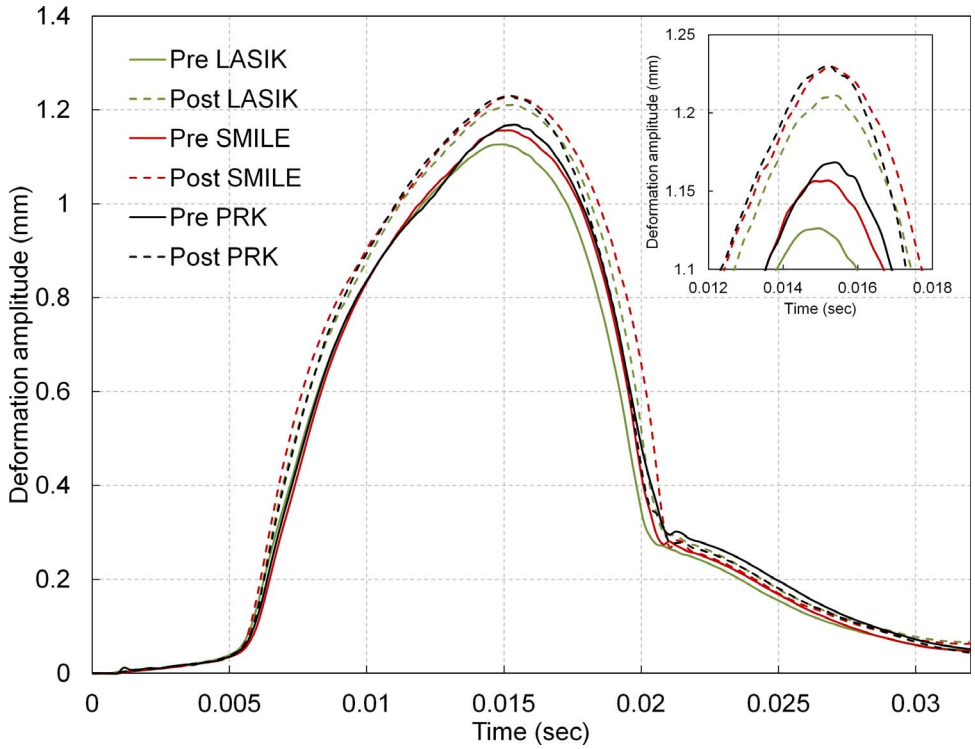

Figure 3. Mean deformation amplitude of a cohort of eyes that underwent LASIK, SMILE, and PRK. *Solid and dotted lines* indicate mean preoperative and postoperative measurement, respectively. The measurement near the peak deformation amplitude is magnified in the *inset box*.

Table 3. Regression Result Between In Vivo Postoperative Measurement (y) and Predicted (x) Postoperative Value for Corneal Stiffness, Peak Deformation, and Peak Deflection Amplitude for Surgical Cohorts (SMILE, LASIK, and PRK) and All Eyes Together. All the Regression Results Tabulated Below Had P Value < 0.001

Group	Parameter	Regression Equation	r
SMILE, $n = 12$	Kc (mean), N/m	$y = 15.05 + 0.81\,x$	0.93
	Kc (constant), N/m	$y = -2.62 + 1.06\,x$	0.95
	Peak deformation amplitude, mm	$y = -0.34 + 1.21\,x$	0.89
	Peak deflection amplitude, mm	$y = -0.08 + 1.0\,x$	0.89
LASIK, $n = 12$	Kc (mean), N/m	$y = 1.74 + 0.98\,x$	0.90
	Kc (constant), N/m	$y = -3.08 + 1.05\,x$	0.93
	Peak deformation amplitude, mm	$y = -0.05 + 1.0\,x$	0.89
	Peak deflection amplitude, mm	$y = 0.42 + 0.57\,x$	0.83
PRK, $n = 12$	Kc (mean), N/m	$y = 7.92 + 0.95\,x$	0.99
	Kc (constant), N/m	$y = 16.93 + 0.86\,x$	0.96
	Peak deformation amplitude, mm	$y = 0.31 + 0.72\,x$	0.89
	Peak deflection amplitude, mm	$y = 0.24 + 0.71\,x$	0.93
All eyes, $n = 36$	Kc (mean), N/m	$y = 7.03 + 0.93\,x$	0.95
	Kc (constant), N/m	$y = 11.11 + 0.91\,x$	0.94
	Peak deformation amplitude, mm	$y = 0.19 + 0.81\,x$	0.87
	Peak deflection amplitude, mm	$y = 0.26 + 0.70\,x$	0.90

As a case example, one eye was chosen from each cohort (discussed above) to demonstrate the predictive ability of the surgical finite element simulations. The preoperative thickness of the LASIK, SMILE, and PRK eye was 515, 500, and 504 μm, respectively. The preoperative IOP of the LASIK, SMILE, and PRK eye was 16, 15, and 18.8 mm Hg, respectively. The preoperative manifest refraction spherical equivalent of the LASIK, SMILE, and PRK eye was –6.13, –6.63, and –7.25 diopter (D), respectively. Figure 4A shows the preoperative deformation amplitude of each eye reported by Corvis-ST. The dotted line represents the deformation estimated by the inverse finite element method. The optimized material properties are listed below:

- LASIK eye: $C_1 = 80.13$ kPa, $C_2 = 2.52$ MPa, $k_1 = 25.1$ kPa, $k_2 = 430.9$, Kz = 1267 N/m, $\mu = 4.61$ Pa.sec and m = 0.03 gm.
- SMILE eye: $C_1 = 82.75$ kPa, $C_2 = 1.98$ MPa, $k_1 = 55.3$ kPa, $k_2 = 637.1$, Kz = 1775 N/m, $\mu = 3.07$ Pa.sec and m = 0.05 gm.
- PRK eye: $C_1 = 68.4$ kPa, $C_2 = 2.62$ MPa, $k_1 = 41.9$ kPa, $k_2 = 706.4$, Kz = 1379 N/m, $\mu = 3.72$ Pa.sec and m = 0.04 gm.

Preoperatively, peak deformation amplitude was 1.12 mm in the LASIK and SMILE eyes. In the PRK eye, it was 1.14 mm. In the LASIK eye, postoperative measured and calculated (finite element simulations) peak deformation amplitudes were 1.42 and 1.42 mm, respectively. The same were 1.30 and 1.32 mm, respectively, in the SMILE eye. In the PRK eye, the same were 1.28 and 1.28 mm, respectively. Preoperatively, Kc (constant) was 105.3, 104.5, and 101.7 N/m, respectively. In the LASIK eye, postoperative measured (in vivo deformation amplitude analyzed with the analytical method) and calculated (finite element simulations) Kc (constant) was 85.4 and 79.5 N/m, respectively. In the SMILE eye, the same were 95.4 and 90.5 N/m, respectively. In the PRK eye, the same were 96.5 and 93.1 N/m, respectively. Thus, the postoperative finite element simulations estimated the peak deformation amplitude better than Kc (constant). Figure 4B shows an overlay of preoperative and postoperative [both measured by Corvis-ST (solid lines) and prediction by surgical finite element models (dotted lines)] deformation amplitude.

Discussion

These are exciting times for the field of refractive surgery since a diverse array of procedures is available to treat refractive error in patients. Biomechanics of the cornea is one of the key drivers of improved techniques.[2–4] SMILE leaves most of the anterior stroma intact, which incidentally is the stiffest region of the stroma. Thus, SMILE caused the least biomechanical changes in the cornea in theoretical models.[3,4] However, clinical evaluation of biomechanical changes cannot be performed in terms of the mechanical stresses and displacements[19] as these parameters cannot be measured in patients yet. Air-puff applanation is the only available technique to clinically evaluate these procedures. Therefore, this study focused exclusively on expected deformation response of the cornea after simulated LASIK, PRK, and SMILE coupled with air-puff applanation. The following were the key outcomes from this study:

- When a cohort of eyes was measured with Corvis-ST before and after surgery, PRK eyes had the least decrease in stiffness parameters. Also, LASIK and SMILE caused a much greater decrease in stiffness parameters (Table 2). However, the change in in vivo peak deformation and deflection amplitude was similar between the cohorts (Table 2). This highlighted the need for patient-specific prediction of deformation amplitude using patient-specific finite element models since theoretical models, devoid of patient-specific material properties, predicted SMILE to cause the least change in corneal stiffness.[3,4]
- PRK eyes had the best agreement between in vivo and predicted postoperative value of stiffness, peak deformation amplitude, and peak deflection amplitude. SMILE and LASIK eyes also had excellent agreement for stiffness parameters (Table 2). Flap or cap could have reduced the level of agreement between in vivo and predicted postoperative value of peak deformation amplitude and peak deflection amplitude in LASIK and SMILE eyes.
- Figures 4A and 4B show the accuracy of determination of deformation amplitude using the finite element simulations and assumptions of wound healing (crimping of collagen fibers) in one eye from each cohort (SMILE,

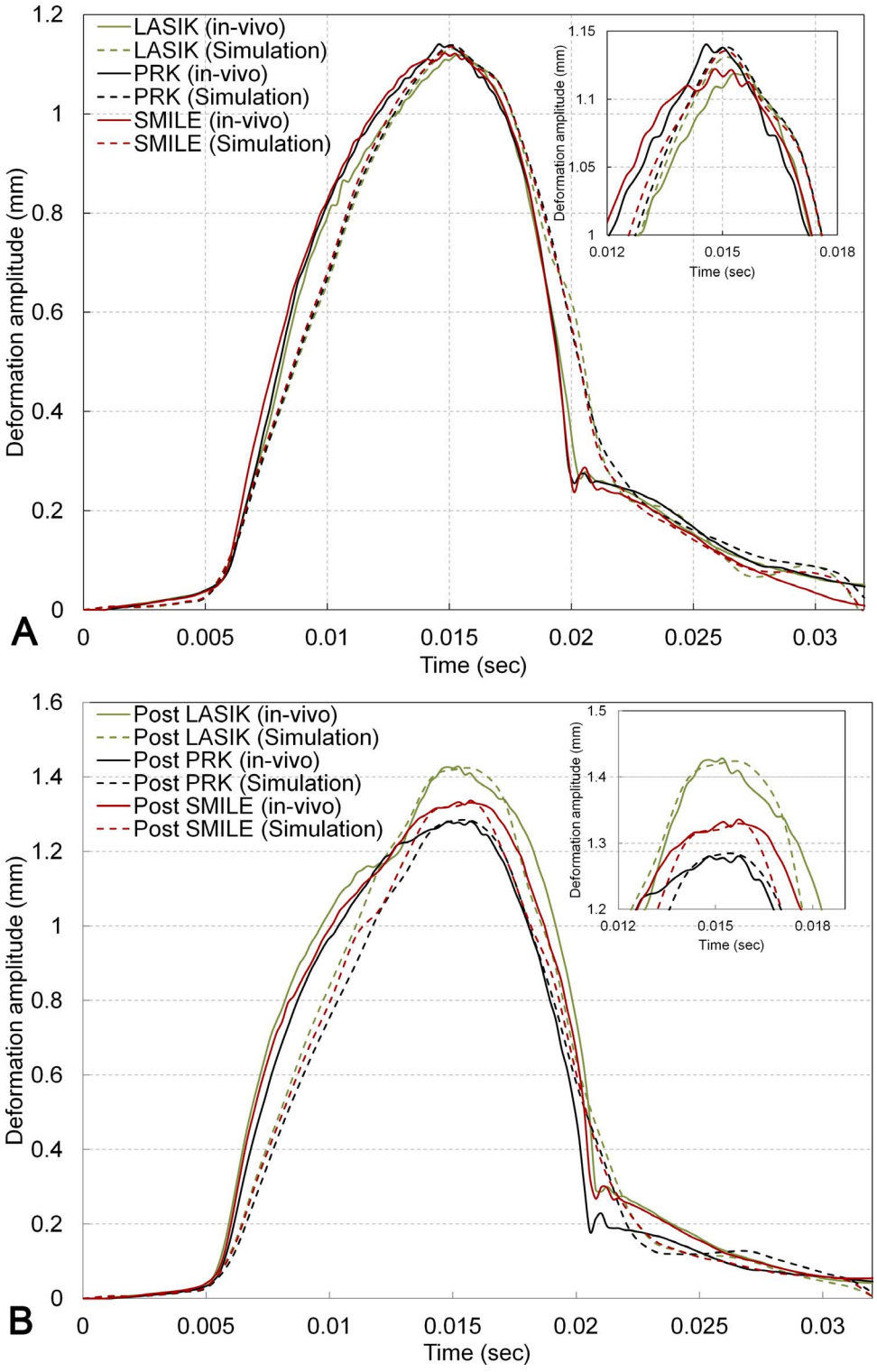

FIGURE 4. (**A**) Mean preoperative deformation amplitude of an individual eye from each cohort (Fig. 3). *Dotted line* shows the computed result of the inverse finite element method. (**B**) Mean preoperative and postoperative deformation amplitude for the same eyes. For the preoperative time points, *dotted lines* show the estimate of the inverse finite element method (same as Fig. 4A). For the postoperative time points, *dotted lines* show the calculated deformation amplitude using the preoperative material properties and finite element simulations of the surgeries.

LASIK, and PRK). Such modeling tools could be integrated with Corvis-ST in future versions of the device.

The study also introduced two variants of remodeling in the flap and cap, which were attributed to short- and long-term response. These variants were derived from recent observations of patient corneas after surgery.[13] The results showed that air-puff deformation response of the cornea was highly dependent on the preoperative material properties of the cornea with the assumption of short-term wound healing

response. Further, for the same treatment, a thicker flap or cap and theoretical models predicted slightly greater stiffness postoperatively.[3,4] Clinical results of comparative studies between LASIK and PRK with the Corvis-ST generally indicate a stiffer biomechanical response after PRK than predicted by the model.[5–7] This indicated the importance of greater degree of fibrotic scars and haze formation in PRK than in LASIK,[20,21] which could have resulted in some biomechanical compensation to removal of the stiffest region of the stroma. Clinical results of comparative studies between LASIK and SMILE using the Corvis-ST indicated similar biomechanical changes.[8–10] This study provided an explanation for these observations and demonstrated the limitation in using device deformation variables such as peak deformation amplitude to compare SMILE and LASIK. Our inverse simulation method of comparing postoperative outcomes may yield better segregation of biomechanical responses after SMILE and LASIK. Future inverse models could benefit with a continuum mechanics approach to simulate the biological stiffening effect after PRK, though this would be a challenging task.

An assumption made in this study was the temporal healing response. A significantly lesser number of collagen lamellae were cut in SMILE compared to LASIK. In a recent study, Bowman's layer distortions returned to preoperative magnitudes in the SMILE eyes within 6 months after surgery.[22] However, the distortions were greater than preoperative magnitudes in the LASIK eyes after surgery.[22] This led us to conclude that crimping in the collagen may not have returned to preoperative levels in the LASIK eyes even after longer healing time. Further long-term follow-up would be required to confirm this trend, but 6-month results lend credence to our modeling assumptions. Another limitation of the study was that the effect of hydration on the elastic strength of the cornea was not evaluated. The deformation amplitude was a dynamic but fast measurement. The deformation amplitude is primarily determined by elastic properties of the cornea.[11,15,16,23] However, the net stress in the fiber would be a vector summation of the stress due to IOP and fluid pressure. If hydration was significantly altered after surgery, then postoperative deformation amplitude could differ significantly from the model predictions; that is, ICC could be lower than 0.9 for all variables.

Another limitation was that a reduced eye model was implemented since patient-specific geometric data on globe, muscles, and fat were not available in the routine clinic. A reduced eye model is also warranted from the perspective of reducing the computational cost without significantly affecting the reliability of the predictions.[11] Further, postoperative epithelium thickness is no longer as uniform as preoperative thickness, and this introduced an approximation to the true thickness of the postoperative stroma. Most current OCT devices limit epithelium thickness reports to the central 6-mm cornea only. Thus, the data were insufficient for inclusion in patient-specific simulations, where the corneal diameter was significantly greater. These limitations could also explain the difference between postoperative corneal stiffnesses derived from in vivo deformation amplitude and the same estimated from simulation results.

Further study with inverse finite element modeling and postoperative measurements on patient corneas can help us to understand this effect. In a previous study, it was shown that the magnitude and distribution of the mechanical stresses in the cap and RSB of the SMILE model were similar to the preoperative equivalent thickness state.[4] The same was not observed in the LASIK model.[4] Thus, SMILE left the residual cornea biomechanically stiffer than LASIK.[4] However, the relation between stress and peak deformation amplitude was not linear; for example, a 10% increase in the stress in the RSB cannot be considered as a 10% increase in peak deformation amplitude. The results from this study show that the alteration in stresses in the postoperative models resulted in minor changes in simulated deformation amplitude. This was in agreement with recent clinical studies comparing biomechanics of SMILE and LASIK with Corvis-ST.[8–10] To conclude, this is the first simulation study to show the predicted deformation amplitude after simulated LASIK, SMILE, and PRK, using novel structural perturbations that may be representative of the in vivo state of the cornea after surgery. Future studies need to investigate alternate analysis techniques or newer measurement techniques to quantify the viscous contribution to in vivo tissue stiffness.

Acknowledgments

Supported in part by a research grant from the Indo-German Science and Technology Center, Government of India, and by Carl Zeiss Meditec, Germany.

Disclosure: **M. Francis**, None; **P. Khamar**, None; **R. Shetty**, None; **K. Sainani**, None; **R.M.M.A. Nuijts**, None; **B. Haex**, None; **A. Sinha Roy**, None

References

1. Winkler M, Shoa G, Xie Y, et al. Three-dimensional distribution of transverse collagen fibers in the anterior human corneal stroma. *Invest Ophthalmol Vis Sci*. 2013;54:7293–7301.
2. Randleman JB, Dawson DG, Grossniklaus HE, McCarey BE, Edelhauser HF. Depth-dependent cohesive tensile strength in human donor corneas: implications for refractive surgery. *J Refract Surg*. 2008;24:S85–S89.
3. Reinstein DZ, Archer TJ, Randleman JB. Mathematical model to compare the relative tensile strength of the cornea after PRK, LASIK, and small incision lenticule extraction. *J Refract Surg*. 2013;29:454–460.
4. Sinha Roy A, Dupps WJ Jr, Roberts CJ. Comparison of biomechanical effects of small-incision lenticule extraction and laser in situ keratomileusis: finite-element analysis. *J Cataract Refract Surg*. 2014;40:971–980.
5. Kamiya K, Shimizu K, Ohmoto F. Comparison of the changes in corneal biomechanical properties after photorefractive keratectomy and laser in situ keratomileusis. *Cornea*. 2009;28:765–769.
6. Hashemi H, Asgari S, Mortazavi M, Ghaffari R. Evaluation of corneal biomechanics after excimer laser corneal refractive surgery in high myopic patients using dynamic Scheimpflug technology. *Eye Contact Lens*. 2017;43:371–377.
7. Hassan Z, Modis L Jr, Szalai E, Berta A, Nemeth G. Examination of ocular biomechanics with a new Scheimpflug technology after corneal refractive surgery. *Cont Lens Anterior Eye*. 2014;37:337–341.
8. Pedersen IB, Bak-Nielsen S, Vestergaard AH, Ivarsen A, Hjortdal J. Corneal biomechanical properties after LASIK, ReLEx flex, and ReLEx smile by Scheimpflug-based dynamic tonometry. *Graefes Arch Clin Exp Ophthalmol*. 2014;252:1329–1335.
9. Shen Y, Chen Z, Knorz MC, Li M, Zhao J, Zhou X. Comparison of corneal deformation parameters after SMILE, LASEK, and femtosecond laser-assisted LASIK. *J Refract Surg*. 2014;30:310–318.
10. Sefat SM, Wiltfang R, Bechmann M, Mayer WJ, Kampik A, Kook D. Evaluation of changes in human corneas after femtosecond laser-assisted LASIK and small-incision lenticule extraction (SMILE) using non-contact tonometry and ultra-high-speed camera (Corvis ST). *Curr Eye Res*. 2016;41:917–922.

11. Sinha Roy A, Kurian M, Matalia H, Shetty R. Air-puff associated quantification of non-linear biomechanical properties of the human cornea in vivo. *J Mech Behav Biomed Mater*. 2015;48:173–182.
12. Mrochen M, Donitzky C, Wüllner C, Löffler J. Wavefront-optimized ablation profiles: theoretical background. *J Cataract Refract Surg*. 2004;30:775–785.
13. Shroff R, Francis M, Pahuja N, Veeboy L, Shetty R, Sinha Roy A. Quantitative evaluation of microdistortions in Bowman's layer and corneal deformation after small incision lenticule extraction. *Trans Vis Sci Tech*. 2016;5(5):12.
14. Grytz R, Meschke G. A computational remodeling approach to predict the physiological architecture of the collagen fibril network in corneo-scleral shells. *Biomech Model Mechanobiol*. 2010;9:225–235.
15. Matalia J, Francis M, Tejwani S, Dudeja G, Rajappa N, Sinha Roy A. Role of age and myopia in simultaneous assessment of corneal and extraocular tissue stiffness by air-puff applanation. *J Refract Surg*. 2016;32:486–493.
16. Matalia J, Francis M, Gogri P, Panmand P, Matalia H, Sinha Roy A. Correlation of corneal biomechanical stiffness with refractive error and ocular biometry in a pediatric population. *Cornea*. 2017;36:1221–1226.
17. Bak-Nielsen S, Pedersen IB, Ivarsen A, Hjortdal J. Repeatability, reproducibility, and age dependency of dynamic Scheimpflug-based pneumotonometer and its correlation with a dynamic bidirectional pneumotonometry device. *Cornea*. 2015;34:71–77.
18. Lopes BT, Roberts CJ, Elsheikh A, et al. Repeatability and reproducibility of intraocular pressure and dynamic corneal response parameters assessed by the Corvis ST. *J Ophthalmol*. 2017;2017:8515742.
19. Seven I, Vahdati A, Pedersen IB, et al. Contralateral eye comparison of SMILE and flap-based corneal refractive surgery: computational analysis of biomechanical impact. *J Refract Surg*. 2017;33:444–453.
20. Dupps WJ Jr, Wilson SE. Biomechanics and wound healing in the cornea. *Exp Eye Res*. 2006;83:709–720.
21. Hjortdal JØ, Møller-Pedersen T, Ivarsen A, Ehlers N. Corneal power, thickness, and stiffness: results of a prospective randomized controlled trial of PRK and LASIK for myopia. *J Cataract Refract Surg*. 2005;31:21–29.
22. Shetty R, Francis M, Shroff R, et al. Corneal biomechanical changes and tissue remodeling after SMILE and LASIK. *Invest Ophthalmol Vis Sci*. 2017;58:5703–5712.
23. Simonini I, Pandolfi A. The influence of intraocular pressure and air jet pressure on corneal contactless tonometry tests. *J Mech Behav Biomed Mater*. 2016;58:75–89.

Investigative Ophthalmology & Visual Science